

Tumorigenesis and Neoplastic Progression

Alterations in Nuclear Pore Architecture Allow Cancer Cell Entry into or Exit from Drug-Resistant Dormancy

Yayoi Kinoshita,* Tamara Kalir,* Jamal Rahaman,[†]
Peter Dottino,[†] and D. Stave Kohtz*[‡]

From the Departments of Pathology,* Obstetrics, Gynecology, and Reproductive Science,[†] and Oncological Sciences,[‡] Mount Sinai School of Medicine, New York, New York

Phenotypic diversity arises in tumors just as it does in developing organisms, and tumor recurrence frequently manifests from the selective survival of divergent drug-resistant cells. Although the expanding tumor cell population may be successfully targeted, drug-resistant cells may persist and sustain the tumor or enter dormancy before igniting a future relapse. Herein, we show that partial knockdown of nucleoporin p62 (NUP62) by small-interfering RNA confers cisplatin resistance to cultured high-grade ovarian carcinoma cells. Treatment with NUP62 small-interfering RNA and cisplatin leaves resistant cells in a state of dormancy; some dormant cells can be induced to proliferate by transient induction of NUP62 expression from an ectopic expression construct. In addition to suggesting functional links between nuclear pore complex architecture and cancer cell survival, the culture system provides a novel experimental window into the dynamics of tumor cell drug resistance and dormancy. (*Am J Pathol* 2012, 180:375–389; DOI: 10.1016/j.ajpath.2011.09.024)

Ovarian cancer is the fifth leading cause of cancer-related deaths among US women; among gynecological tumors, it most frequently results in death.¹ The prevailing treatment for ovarian cancer is surgical debulking, followed by platinum-based chemotherapy. Although ovarian carcinomas initially respond well to treatment with platinum salts, such as cisplatin, most recur, a course that is also followed by other tumor types. Modulation of drug uptake and efflux, enhanced mechanisms of detoxification, inhibition of apoptosis, and recovery or enhancement of DNA repair mechanisms² have been associated with enhanced survival of tumor cells challenged with platinum salts. Although the mechanisms of tumor cell escape from cisplatin are not well

understood, alterations in genes or gene products with diverse functions may influence sensitivity to platinum salts, including metallothionein (an intracellular metal sink³), CCND1 (a G₁ cyclin⁴), ERCC1 (an enzyme involved in DNA excision repair^{5,6}), glutathione S-transferase (thought to modulate signal transduction kinase cascades in response to stress⁷), IL-6 (a cytokine⁸), and type IV collagen.⁹ In certain cultured ovarian carcinoma cells, modulators of apoptosis, including p53,^{10–12} X-linked inhibitor of apoptosis protein,^{13,14} and Akt,^{15,16} work as interdependent determinants in the response to platinum salts.¹⁷ Rather than being determinants of response to therapeutic challenge, however, p53 mutations appear almost ubiquitously and appear to function as early or driver mutations in high-grade ovarian carcinomas.^{18,19}

The recurrence of tumors from remnant tumor cells presents an important challenge to the success of cancer chemotherapy. Adding to the complexity of this challenge, drug resistance of remnant tumor cells can be conferred by ephemeral epigenetic variability that is obscured on recurrence of the tumor. A review²⁰ of retreatment of relapsed tumors of different types revealed that transient resistance to chemotherapy is common, and the authors statistically discounted somatic mutation as the prevailing mechanism, suggesting instead epigenetic modalities. A study²¹ of retreatment of patients with ovarian cancer with platinum drugs after remission and relapse with the same regimen of chemotherapy revealed surprisingly high probabilities of success. Analogously, in some animal models, growth of remnant cells does not result in the appearance of resistant tumors; rather, it results in the growth of tumors that, when

Supported by grants from the NIH/National Cancer Institute (1R03CA141318) and the Ruttenberg family. Microscopy was performed at the Mount Sinai School of Medicine Microscopy Shared Resource Facility, which is supported by a shared resources grant from the NIH/National Cancer Institute (5R24 CA095823-04), a major research instrumentation grant from the National Science Foundation (DBI-9724504), and a shared instrumentation grant from the NIH (1 S10 RR0 9145-01).

Accepted for publication September 22, 2011.

Address reprint requests to D. Stave Kohtz, Ph.D., Department of Pathology (1194), Mount Sinai School of Medicine, One Gustave Levy Place, New York, NY 10029. E-mail: stave.kohtz@mssm.edu.

treated, consist of another population of cells that respond similarly to the untreated tumor.^{2,22} Recent studies²³ of tumor cells in culture have shown that populations of drug-tolerant cells persist after treatment with different chemotherapeutic agents and that these cells are mostly quiescent and express surface markers in common with cancer stem cells. When these cells remain in culture in the presence of drug, a fraction produce colonies of cells with relatively stable tolerance; that cell population remains tolerant in the presence of drug and for many generations after drug removal. The frequency with which tolerant and stably tolerant cells appeared in these experiments also suggests mechanisms that do not involve genetic mutations. Further studies²³ indicated that chemical agents that inhibit histone demethylation also block acquisition of drug tolerance, suggesting an epigenetic mechanism.

The functions of the nuclear pore complex (NPC) in nucleocytoplasmic transport and chromatin organization make it a potential nexus for control of normal and cancer cell phenotypes. The NPC assembles in a modular form from multiples of eight nucleoporin (NUP) subcomplexes (as visualized²⁴ and modeled²⁵), with a central framework consisting of a symmetric pair of central inner rings (containing NUP107-160 subcomplexes²⁶). Asymmetric annular rings line the cytoplasmic (containing the NUP88-NUP214 subcomplex^{27,28}) and nuclear (containing NUP153²⁹) faces of the pore, whereas asymmetric filamentous structures project from the annular rings into the nucleus (containing NUP153-Tpr²⁹) or cytoplasm (containing NUP358³⁰). The NUP62 subcomplex, which contains the FG-repeat NUP62,³¹ forms two rings on the inner channel of the pore.^{32,33} Although the major framework components of the NPC are generally static and rigid, the FG-repeat-containing NUPs, which include NUP62, NUP98, NUP153, and NUP358, mediate transport of cargo and karyopherins by interacting dynamically with the NPC and exploiting their own structural plasticity.³⁴ A subset of the FG-repeat-containing NUPs (including NUP62) function in transcriptional regulation at intranuclear sites distal to the NPC.^{35,36} Interactions with FG-repeat and possibly other NUPs appear to play a role in chromatin organization at the nuclear envelope or within the nucleus.^{36,37}

We have observed that knockdown of NUP62 results in growth retardation of several cell lines, including cells derived from a high-grade ovarian carcinoma (TOV112D) that we chose to study further. The TOV112D cell line was generated before chemotherapy or radiation therapy from a tumor displaying endometrioid histological features and an extremely aggressive disease course.³⁸ Correspondingly, the cells are rapid growing and display a high frequency of colony formation in semisoft medium and of tumor formation in nude mice.³⁸ Recent studies³⁹⁻⁴¹ have shown that p53 mutations are present in most high-grade ovarian carcinomas with either serous or endometrioid histological characteristics; consistent with other tumors of the same lineage, TOV112D cells possess a mutant p53 genotype.³⁸ We will show that knockdown of NUP62 pauses cells upstream of the G₁-S-phase border and confers resistance to cisplatin through a mechanism that appears to require enrichment of NPCs lacking NUP62. This contrasts with other agents that pause progression in the G₁ or G₂ phase of

the cell cycle and enhance sensitivity to the cytotoxic effects of cisplatin.⁴²⁻⁴⁸ Knockdown of NUP62 in the presence of cisplatin leaves surviving cells in a state resembling cellular dormancy,⁴⁹ and spontaneous colonial proliferation of the apparently dormant cells was observed only rarely in long-term cultures. In contrast, transient induction of NUP62 expression pushed resistant cells out of dormancy, resulting in rapid colonial expansion. The modulation of nuclear pore architecture represents a novel mechanism through which tumor cells could acquire transient resistance to certain chemotherapeutic agents, and the culture system represents a dynamic and controlled experimental tool for studying entry into and emergence from cancer cellular dormancy.

Materials and Methods

Cell Lines

The human ovarian carcinoma cell line TOV112D was obtained from American Type Culture Collection (Manassas, VA). Cultures were maintained in Dulbecco's modified Eagle's medium (Cellgro, Manassas, VA) supplemented with 10% to 15% fetal bovine serum (tetracycline free for TOV112D-CAP cells).

Antibodies

Antibodies to NUP62 (sc-25523; Figure 1), C23 (nucleolin, sc-8031), cyclin E (sc-198), and cyclin A (sc-751) were obtained from Santa Cruz Biotechnology (Santa Cruz, CA). Antibody to NUP160 (A301-790A) was obtained from Bethyl Laboratories (Montgomery, TX). Antibody to NUP133 (H00055746-M01) was obtained from Abnova (Walnut, CA). Monoclonal antibody (MAB) 414 (MMS-120R) was obtained from Covance (Princeton, NJ). Antibody to NUP62 conjugated to fluorescein isothiocyanate (611962) was obtained from BD Biosciences (San Jose, CA). Phosphorylated histone H3 (Ser10) antibody (06-570) was obtained from Upstate Biotechnology (Millipore, Billerica, MA). Antibody to glyceraldehyde-3-phosphate dehydrogenase (GAPDH; MAB374) was obtained from Chemicon (Millipore). All secondary antibodies for immunofluorescence microscopy were obtained from Jackson ImmunoResearch Laboratories (West Grove, PA).

Immunofluorescence Microscopy

Subconfluent cells were cultured on glass coverslips. Immunofluorescence staining was performed similarly to that performed by Maeshima et al.⁵⁰ Cells were fixed with 3.7% paraformaldehyde in PBS and quenched with 50 mmol/L glycine in HMK buffer (20 mmol/L HEPES, pH 7.5; 1 mmol/L MgCl₂; and 100 mmol/L KCl). Coverslips were briefly washed with HMK. After cells were treated with 0.5% Triton X-100 in HMK, they were treated with blocking solution (10% normal donkey serum and 1% bovine serum albumin in HMK buffer). Cells were incubated with primary antibody for 1 to 2 hours at room temperature or overnight at 4°C. After washing with HMK five times, the

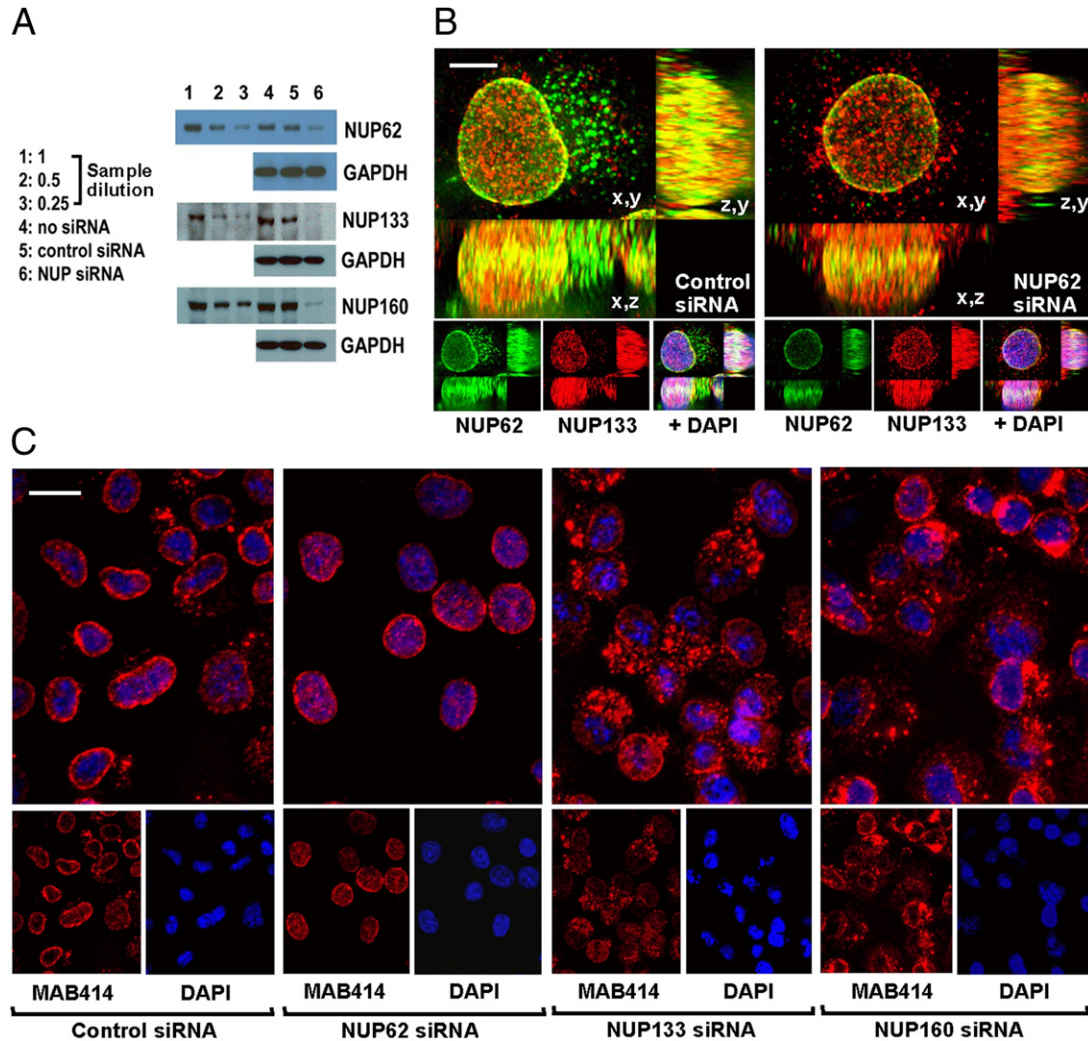


Figure 1. Knockdown of NUP62 reduces NUP62 immunolabeling but does not ablate NPCs. **A:** Western blot analyses of NUP62, NUP133, and NUP160 knockdown by siRNA treatment of TOV112D cells. Dilutions of control siRNA sample (lanes 1 to 3) correlate the reductions in signal intensity with fraction of protein reduction. **B:** Immunofluorescence microscopy of NUP62 and NUP133 in control and NUP62 siRNA-treated TOV112D-9 cells. Optical sections ($\times 63$, oil immersion) were taken at 250-nm intervals and merged, and images projected from three planes (x,y; x,z; and z,y) are shown. Scale bar = 5 μm . **C:** MAB414 immunofluorescence microscopy of TOV112D-9 cells treated with control, NUP62, NUP133, or NUP160 siRNA. Optical sections ($\times 40$, air) were taken at 500-nm intervals and merged. Accumulation of cytoplasmic annulate lamellae in cells treated with NUP133 or NUP160 siRNA resulted after NPC disruption. Scale bar = 10 μm .

cells were incubated with secondary antibodies (Jackson ImmunoResearch). Cells were washed in PBS and mounted with VectaShield mounting medium with DAPI (Vector Laboratories, Burlingame, CA). Bright-field microscopy was performed using a Zeiss Axioplan 2 microscope (Carl Zeiss Microscopy, LLC, Thornwood, NY). Images were acquired with either $\times 40$ (air) or $\times 63$ (oil) objectives in Z-stack series extending 10 to 15 μm . Bright-field images were compiled after three-dimensional deconvolution (AutoQuant; MediaCybernetics, Bethesda, MD) and projection.

Western Blot Analyses

Cell lysates were prepared by washing adherent cells once in PBS, followed directly by lysis in SDS sample buffer (62.5 mmol/L Tris-HCl, pH 6.8; 10% glycerol; 2% SDS; 5% β -mercaptoethanol; and 125 $\mu\text{g}/\text{mL}$ bromophenol blue). SDS-PAGE and transfers of proteins to nitrocellulose membranes

were performed as described by the Amersham ECL Plex Western blotting system (GE Healthcare, Pittsburgh, PA). Membranes were scanned by the Typhoon Trio (GE Healthcare) and analyzed with ImageQuant TL (GE Healthcare) or developed using the Amersham ECL Western blotting system (GE Healthcare).

Assembly and Transfection of Tetracycline-Inducible NUP62 Expression Constructs

A 1569-bp NheI/HindIII fragment containing the human NUP62 cDNA (cDNA clone MGC: 119675; IMAGE: 40011537; the full-length human NUP62 protein) was cloned into the NheI/HindIII site of pTRE-Tight-BI-DsRed2 DNA vector (Clontech, Mountain View, CA) to make pTRE-Tight-BI-DsRed2-NUP62. Construct integrity was confirmed by DNA sequence analysis. Cells were plated at 70% to 80% confluency 24 hours before transfection. Transfections were performed by the calcium phosphate

method. The tetracycline-inducible target cell line TOV112D-9 was derived from TOV112D by stable transfection with pTet-On (Tet-On Gene Expression Systems; Clontech). The Ase I-linearized pTRE-Tight-BI-DsRed2-NUP62 was stably transfected into TOV112D-9 cells by cotransfection with pIND/Hygro and selection with 200 $\mu\text{g}/\text{mL}$ Hygromycin B to generate TOV112D-CAP cells. Selected clones were cultured in tetracycline-free fetal bovine serum and induced to express NUP62 with 2 to 4 $\mu\text{g}/\text{mL}$ doxycycline hyclate. Regulated expression was verified by immunoblot analysis.

Knockdown by siRNA Transfection

Cells were plated at $3 \times 10^4/\text{cm}^2$ using 10% fetal bovine serum in Dulbecco's modified Eagle's medium without the addition of antibiotics for 24 hours. Cells were transfected with small-interfering RNA (siRNA) using Lipofectamine RNAiMAX (Invitrogen, Carlsbad, CA) and the manufacturer's recommended procedure. The siRNAs for NUP62 (sc-36107), NUP133 (sc-60035), NUP160 (sc-106318), control siRNA-A (sc-37007), and control siRNA-B (sc-44230) were obtained from Santa Cruz Biotechnology.

Cisplatin Resistance and Survival Assays

Subconfluent cells were transfected with control or NUP siRNAs and incubated for 24 hours. Cisplatin (EMD4 Biosciences, Darmstadt, Germany) was then added at a different concentrations to some cultures for 48 hours in the continuing presence of the siRNAs. Live cells were identified by Trypan blue exclusion and counted. TOV112D-9 or TOV112D-CAP cells were plated at 30×10^4 cells per well on six-well plates in 10% tetracycline-free fetal bovine serum in Dulbecco's modified Eagle's medium without antibiotics. The cells were treated with 2 to 4 $\mu\text{g}/\text{mL}$ doxycycline to induce expression of NUP62.

Cell Cycle Analyses

For fluorescence-activated cell sorter (FACS) analyses, cells were harvested after trypsin treatment and trypsin inactivation in serum-containing medium. Harvested cells were rinsed with PBS once, resuspended in PBS containing 5 mmol/L EDTA, fixed in ice-cold 70% ethanol by the addition of absolute ethanol dropwise while lightly vortex mixing, and incubated for at least 30 minutes at 4°C. Fixed cells were rinsed in 5 mmol/L EDTA in PBS twice to remove ethanol and resuspended in 5 mmol/L EDTA and 1% bovine serum albumin in PBS. Cells were treated with RNase A (Sigma-Aldrich, St. Louis, MO) and 0.1% Nonidet P-40 in PBS for 1 hour and stained with propidium iodide solution (Sigma-Aldrich). An FACScan fitted with CellQuest software and a BD LSR II laser with Diva software (BD Biosciences) were used for analytical flow cytometry. For cell sorting, cells were stained with Vybrant DyeCycle Green stain (V35004 from Invitrogen) and processed with the MoFlo sorter (Beckman Coulter, Inc., Indianapolis, IN).

Cell cycle arrest was achieved by 24-hour incubation of subconfluent cells with 2 $\mu\text{g}/\text{mL}$ aphidicolin. Cells were rinsed with medium once and released in fresh medium

lacking aphidicolin (0 hour), and time points were taken hourly. Cell cycle progression was verified by FACS analysis. Cell lysates were analyzed by using Western blot analysis. Total protein loading was standardized by Coomassie blue staining analysis of samples. Signal intensities were determined by densitometry and normalized to GAPDH or nucleolin, as indicated.

Electron Microscopy and Quantification of Pore Diameters

Tissue samples were immediately fixed in buffered formalin on removal in the operating room and routinely processed. Ultrathin sections were mounted on grids. Sections were viewed using a Jeol (Peabody, MA) 1200 EX electron microscope equipped with an Advanced Microscopy Techniques (Woburn, MA) digital camera. Electron micrographs were taken at $\times 50,000$ and imported into an image morphometry system (NeuroLucida; MicroBrightField, Inc., Williston, VT) for making and obtaining measurements at a print magnification of $\times 209,000$. Pore external diameters, defined by marginated heterochromatin, and internal diameters were digitally imaged. A total of 423 pores were measured.

Immunohistochemical Data

Formalin-fixed, paraffin-embedded sections were cut (5 μm thick) and attached to slides. Removal of paraffin, rehydration, and treatment with hydrogen peroxide were performed as previously described.⁵¹ Antigen retrieval was performed by treated sections with 10 mmol/L citrate buffer (pH 6.0) for 4 minutes at 125°C in a pressure cooker. After cooling, slides were rinsed with PBS. Sections were incubated for 2 hours at 22°C with primary antibody diluted in PBS containing 1% bovine serum albumin and 5% goat serum. The Ultravision LP Detection System was used as a second antibody and for development, according to the manufacturer's specifications (Thermo Fisher Scientific, Waltham, MA). Tumor samples were obtained from archival materials of the Department of Pathology, Mount Sinai School of Medicine (New York, NY), that have been collected with Institutional Review Board approval, as applicable. All fresh tumor samples were de-identified before analysis; hence, the studies using these samples are not considered human subject research by the U.S. Department of Health and Human Services.

Colony Staining

Colonies were rinsed with PBS, then fixed at -20° for 5 minutes with paraformaldehyde (3.7% formalin, 70% ethanol, and 5% acetic acid, brought to volume with normal saline). Colonies were then rehydrated with several changes of water and stained with 0.15% crystal violet.

Results

Partial Knockdown of NUP62 Alters NPC Composition

We first asked whether siRNA-mediated knockdown of NUP62 overtly alters the abundance of NPCs in the nuclear envelope of TOV112D cells. The TOV112D cell line was modified to express the tetracycline transcriptional activator by DNA-mediated transfection of pTet-On, an expression construct for the positive tetracycline transactivator protein (Clontech) to generate TOV112D-9 cells. Several preliminary titration experiments were performed to establish appropriate conditions for siRNA-mediated knockdown of NUP62, NUP133, and NUP160. Conditions were selected that result in 75% to 90% reductions in the total cellular accumulation of the NUPs without affecting accumulation of GAPDH (Figure 1A). Knockdown of NUP62 under these conditions resulted in reduction of NUP62 immunolabeling in NPCs on the nuclear envelope and among cytoplasmic annulate lamellae, whereas double-immunolabeling experiments revealed that the abundance or distribution of NUP133 (a component of the inner core of the NPC) was not altered (Figure 1B). The absence of changes in the immunolabeling pattern of NUP133 suggests that removal of NUP62 does not disrupt nuclear pores or overtly alter their distribution. The images shown in Figure 1, B and C, are projections of merged optical sections rather than a single section, and reveal NUP signals derived from NPCs on planes through the entire nucleus, including the equatorial ring (observed when viewing a single central section of the nucleus) and the dorsal/ventral surfaces (Figure 1B; x,y; x,z; z,y).

Knockdown of either of two inner ring complex proteins (NUP107 or NUP133) has removed NPCs from the nuclear envelope, accompanied by down-regulation of some inner complex proteins and accumulation of other NUPs in the cytoplasm as annulate lamellae.^{52–54} Similarly, we show that, using the conditions used herein, knockdown of NUP133 and of another inner ring complex protein, NUP160, denudes the nuclear envelope of NPCs, accompanied by accumulation of FG-repeat-containing NUPs (detected by the FG-repeat-directed antibody, MAB414⁵⁵) in cytoplasmic annulate lamellae (Figure 1C). Knockdown of NUP160 will be used to disrupt NPCs in experiments described later. In contrast to NUP133 and NUP160, knockdown of NUP62 under the same conditions did not disrupt NPCs, although a weaker signal was observed in some cells because NUP62 (an FG-repeat protein) is one of the antigenic targets of MAB414 (Figure 1C). Together, the data suggest that partial knockdown of NUP62 does not disrupt NPCs or cause cytoplasmic dispersal of FG-repeat proteins; rather, it results in accumulation of NUP62-depleted NPCs.

NUP62 Protein Accumulation Displays a Peak in the Early G₁ Phase of the Cell Cycle

Cultures of TOV112D-9 cells were blocked at the late G₁-S phase of the cell cycle by aphidicolin, then re-

leased. At 1-hour intervals after release, cells were analyzed for DNA content by FACS analysis and for expression of NUP62, cyclin A, cyclin E, phosphorylated histone H3 (phosphoserine 10), nucleolin, and GAPDH by using Western blot analysis. As shown by FACS analysis of DNA content, TOV112D-9 cells are paused in late G₁-S by aphidicolin (Figure 2A, 0 hour); after aphidicolin is removed, the cells rapidly enter the S phase (Figure 2A, 3 hours) and proceed to G₂ (Figure 2A, 9 hours), then proceed through the G₂ and M phases to return to G₁ (Figure 2A, 18 hours). Intense phosphorylation of histone H3 at serine 10 indicates cells proceeding through the late G₂ and M phases of the cell cycle.⁵⁶ In somatic cells, up-regulation of cyclin A is observed during the S phase, whereas cyclin E expression peaks during progression through G₁ and the G₁-S boundary, and is attenuated during the S phase.⁵⁷ Consistent with the FACS analysis, a peak of cyclin A expression was observed between 2 and 9 hours (S phase), a peak of phosphorylated histone H3 was observed between 9 and 14 hours (G₂-M), and two peaks of cyclin E expression were observed (0 to 2 and 18 to 20 hours for G₁-early S and approaching mid-G₁, respectively). The expression of NUP62 (reported as the 62-kDa band bound by MAB414) was observed to peak in the early G₁ phase of the cell cycle (16 to 19 hours), accompanying the decline in phosphorylated histone H3 and preceding the second peak of cyclin E expression (Figure 2B). The expression of NUP62 was normalized against GAPDH (cytoplasmic protein) and nucleolin (nuclear protein). In both cases, a peak in NUP62 accumulation was observed in the early G₁ phase of the cell cycle (Figure 2C).

Equivalent total protein samples from whole cell lysates made 3, 8.5, and 17.5 hours after release from aphidicolin block were analyzed by using Western blot analysis for NUP62 accumulation. Because levels of protein accumulation do not vary linearly with band intensities in Western blot analyses, these samples were processed on the same blot as a series of whole cell lysate dilutions (Figure 2D). By comparison to the dilution series, the NUP62 amounts accumulated in 3- and 17.5-hour samples appear to differ by approximately twofold. Proliferating TOV112D-9 cells were also stained for DNA content with membrane-permeable Vibrant DyeCycle Green (Invitrogen); sorted by DNA content into G₁, S, and G₂-M populations; and loaded at equal cell numbers per lane for Western blot analysis (Figure 2D). In this analysis, increased accumulation of NUP62 is observed in the G₂-M population. In this type of analysis, the transient peak of NUP62 accumulation in early G₁ is averaged into the signal from the whole G₁ population. The larger total nuclear mass of cells in the G₂-M phase also could contribute to the enhanced NUP62 signal observed in cells at that phase, particularly when loading according to total cell number. FACS analyses of DNA content and NUP62 immunofluorescence revealed peaks of NUP62 signal in fractions of cells in the G₁ and G₂-M phases. Together, these observations suggest the possibility that enhanced accumulation of NUP62 may begin before the completion of abscission during late cytokinesis and may extend into the early G₁ phase. This interpretation also would be

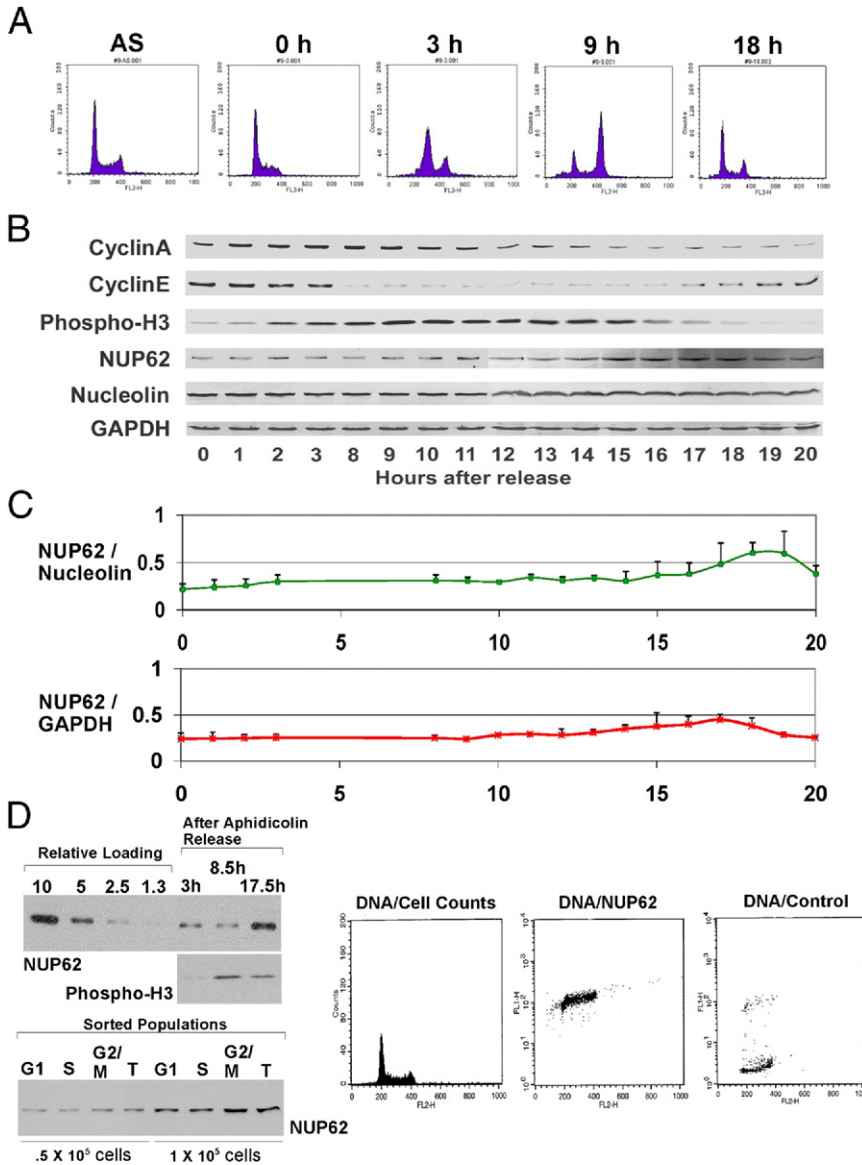


Figure 2. NUP62 accumulation in TOV112D cells peaks in the early G₁ phase of the cell cycle. **A:** FACS analysis of TOV112D-9 cells after release from aphidicolin block. DNA was stained quantitatively with propidium iodide. AS, asynchronously growing culture; 0 hours (h), culture immediately before release; 3 h, culture 3 hours after release; 9 h, culture 9 hours after release; 18 h, culture 18 hours after release. **B:** Western blot analysis of cyclins A and E, phosphorylated histone H3 (Phospho-H3), NUP62 (using MAB414), nucleolin, and GAPDH in whole cell lysates of TOV112D-9 cells at selected times after release from aphidicolin block. **C:** Densitometry analyses of NUP62 signals normalized to nucleolin or GAPDH. Mean values from three experiments were normalized to reflect the same combined signal for all points; means for each point are shown with SDs. **D: Left top panel:** Whole cell lysates were generated at the indicated time points after aphidicolin block, loaded at equivalent total protein, and analyzed by using Western blot analysis for NUP62 and Phospho-H3. A series of dilutions of TOV112D-9 cell whole cell lysates analyzed on the same Western blot with NUP62 antibody is shown for comparison. **Left bottom panel:** Proliferating TOV112D-9 cells were sorted using Vibrant DyeCycle Green stain (Invitrogen) into G₁, S, and G₂-M phases (T refers to the total population), and whole cell lysates derived from 0.5 × 10⁵ or 1 × 10⁵ cells (as indicated) were loaded per lane for Western blot analysis with NUP62 antibody. **Right panel:** FACS analyses of proliferating TOV112D-9 cells, showing DNA content (propidium iodide stain) versus cell count (DNA/Cell Counts), DNA content versus NUP62 immunofluorescence (DNA/NUP62), and DNA content versus background fluorescence (DNA/Control).

consistent with the observation that increased NUP62 accumulation commences as phosphorylation of histone H3 is declining.

Modulation of NUP62 Levels Is Required for Progression through the G₁ Phase of the Cell Cycle

The siRNAs were used to partially knock down NUP62 expression in TOV112D-9 cells, as previously described. Subconfluent TOV112D-9 cells were treated with NUP62 and control siRNAs, then analyzed for DNA content and cell cycle distribution by FACS analysis. Partial knock-down of NUP62 by siRNA resulted in accumulation of cells in the G₁ compartment of the cell cycle (Figure 3A). Removal of NUP62 siRNA from arrested cultures results in the gradual recovery of the nominal growth rate over a few days. The TOV112D-9 cells were further engineered by DNA-mediated transfection of a construct containing a tetracycline activator-induced promoter (TRE) driving ex-

pression of human NUP62 cDNA (pTRE-Tight-BI-DsRed2-NUP62, derived from pTRE-Tight-BI-DsRed2; Clontech). The selected cell line (TOV112D-CAP) over-expresses NUP62 when doxycycline is added to the medium (Figure 3B). The TOV112D-CAP cells were used to analyze the effects of forced NUP62 overexpression on cell cycle distribution. Although a reduction in the rate of cell accumulation was observed in the doxycycline-induced cultures, a comparison of the FACS profiles of cultures with and without doxycycline did not reveal growth arrest in a specific phase of the cell cycle. Rather, the accumulation of signal in the <2N compartment of the induced cultures indicated that overexpression of NUP62 resulted in reduction of the G₁ phase peak and induction of apoptosis in some cells (Figure 3C). Together, the data provide evidence that both up- and down-modulations of NUP62 accumulation, and its putative impact on the architecture of NPC populations, are required for successful transit across the G₁ phase.

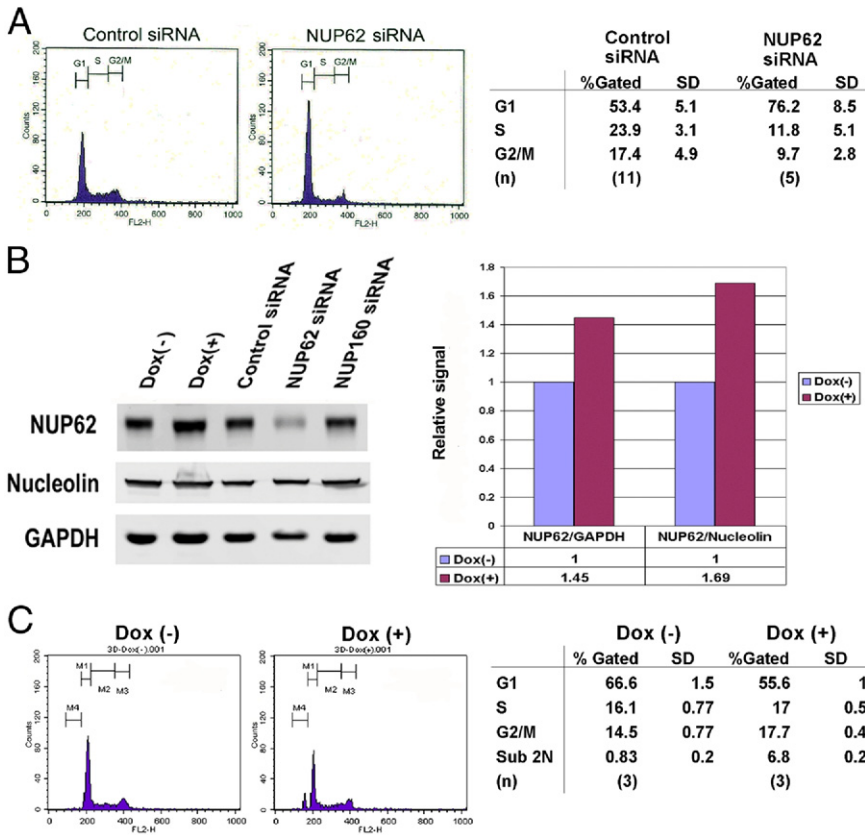


Figure 3. Modulation of NUP62 levels is required for progression through the G₁ phase in TOV112D cells. **A:** FACS analysis of TOV112D-9 cells treated with control or NUP62 siRNA. DNA was stained quantitatively with propidium iodide. Data on the right indicate percentage of cells (mean values) in each gated phase. **B: Left panel:** Western blot analysis of NUP62 expression in TOV112D-CAP cells. Cultures of TOV112D-CAP cells lacking doxycycline [Dox(-)], supplemented with doxycycline for 48 hours [Dox(+)], or lacking doxycycline and treated with control, NUP62, or NUP160 siRNA. **Right panel:** Western blot signals were quantified, and NUP62 signal was normalized, against signals for GAPDH or nucleolin. **C:** FACS analyses of TOV112D-CAP cells cultured in the presence [Dox(+)] or absence [Dox(-)] of doxycycline. DNA was stained quantitatively with propidium iodide. Data on the right indicate percentage of cells (mean values) in each gated phase.

The period of G₁ phase in which progression is paused by knockdown of NUP62 was further resolved. The TOV112D-9 cells were blocked in the late G₁-S phase by incubation with aphidicolin for 24 hours, and then incubated with NUP62 siRNA and aphidicolin for a further 24 hours. At 48 hours, the cells were cultured in medium containing only NUP62 siRNA. After removal of the

aphidicolin block, virtually all of the cells progressed through the S and M phases, even in the continuing presence of NUP62 siRNA (Figure 4A). This result indicates that down-regulation of NUP62 blocks cell cycle progression through an earlier period in the G₁ phase, upstream of the aphidicolin block at late G₁-S. To support this conclusion, cells were incubated with NUP62 siRNA

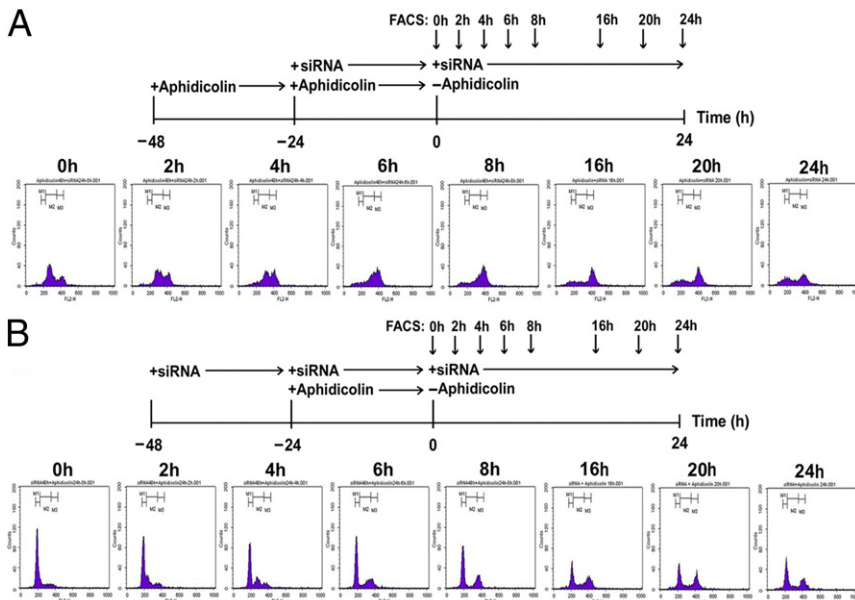


Figure 4. Knockdown of NUP62 specifically restricts progression through the G₁ phase upstream of the G₁-S transition. **A:** Cells released from aphidicolin block proceed through the cell cycle in the presence of NUP62 siRNA. The sequence of events is traced in the top diagram: Cells were incubated with aphidicolin 48 hours (h) before release; 24 h before release, NUP62 siRNA was added; at 0 h, cells were released from aphidicolin block but continued in the presence NUP62 siRNA. FACS analysis results of propidium iodide binding at 0 hours and the times indicated after release are shown. **B:** Many cells treated with NUP62 siRNA are restricted from progressing to an aphidicolin block. The sequence of events is traced in the top diagram: Cells were incubated with NUP62 at 48 h before release; 24 h before release, aphidicolin was added; at 0 h, cells were released from aphidicolin block but remained in the presence NUP62 siRNA. FACS analyses of propidium iodide binding at 0 hours and the times indicated after release are shown.

for 24 hours, then with aphidicolin and NUP62 siRNA for a further 24 hours. At 48 hours, the cells were changed to medium containing only NUP62 siRNA. In this experiment, a peak of cells remained blocked in G₁ by down-regulation of NUP62, even after the removal of aphidicolin (Figure 4B), suggesting that the NUP62 siRNA block precedes that of aphidicolin. However, a small, discrete population of cells also was observed to enter the S phase after removal of aphidicolin. Because NUP62 siRNA knocks down NUP62 accumulation only partially, the block to cell cycle progression is not absolute and most likely behaves similarly to a weir. Although the rate of accumulation is reduced, a few cells accumulate sufficient NUP62 to spill over the weir, only to be blocked at the G₁-S boundary by aphidicolin. When aphidicolin is removed, this discrete group of cells progresses synchronously through the S phase as is evident 4 hours after release (Figure 4B).

Partial Knockdown of NUP62 Confers Resistance to Cisplatin

Because some agents that pause cell cycle progression enhance sensitivity to cisplatin, we queried whether partial knockdown of NUP62 affects the cytotoxic response of cultured ovarian carcinoma cells to cisplatin treatment. The TOV112D-9 cell line was grown in the presence of NUP62 or control siRNA for 24 hours (to 60% to 80% confluence), then treated with different concentrations of cisplatin for 48 hours (continuing in the presence of NUP62 siRNA). In contrast to the reported effects of other inhibitors of cell cycle progression, siRNA-mediated knockdown of NUP62 enhanced survival of cells treated with cisplatin and conferred resistance to higher concentrations of the drug (Figure 5A). The data shown were collected at 48 hours after adding cisplatin; although the survival of cells remaining after treatment with >4 μg/mL cisplatin for ≥48 hours was greatly enhanced by treatment with NUP62 siRNA, the remaining cells entered a period of protracted growth arrest and continued to die off slowly, even after cisplatin was removed (described later). Further experiments revealed that protection against cisplatin cytotoxicity is conferred by the generation of NUP62-depleted nuclear pores, rather than by the loss of an autonomous function of NUP62. For counting, viable cells were distinguished by exclusion of trypan blue. As previously shown, knockdown of NUP160 greatly reduces the density of pores in the nuclear envelope; however, it does not reduce the sensitivity of cells to cisplatin, with TOV112D-9 cells treated with NUP160 siRNA displaying a dose-response to cisplatin after 48 hours similar to cells treated with control siRNA (Figure 5B). Knockdown of both NUP160 and NUP62 abrogated the ability of NUP62 knockdown alone to promote survival of cells in cisplatin (Figure 5B), suggesting that accumulation of NUP62-depleted nuclear pores is required to confer drug resistance.

We queried whether selection of cultured cells with cisplatin results in accumulation of cells expressing less NUP62. Cells that recovered after selection with 4 μg/mL of cisplatin for 48 hours displayed detectable resistance

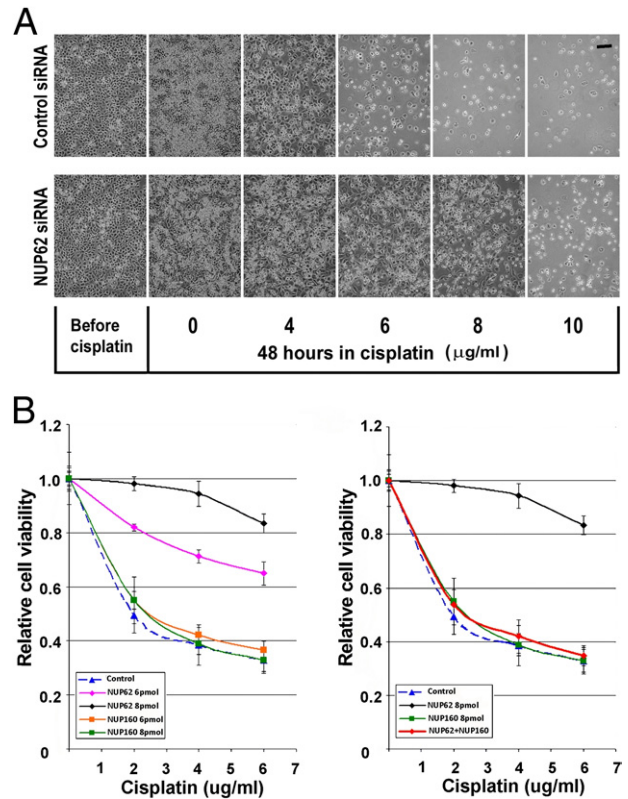


Figure 5. Knockdown of NUP62 confers cisplatin resistance in TOV112D-9 cells. **A:** Phase microscopy of TOV112D-9 cells treated with either control or NUP62 siRNA for 24 hours, then treated with the indicated concentration of cisplatin for 48 hours. Scale bar = 100 μm. **B:** Cells were treated with control, NUP62, NUP160, or a combination of NUP62 and NUP160 siRNAs for 24 hours, then cisplatin was added, and cell counts were taken 48 hours after adding cisplatin. Different quantities of NUP62 and NUP160 siRNA were added to 600-μL cultures (indicated in pmol). The SEs are shown for multiple wells in a single experiment; all experimental determinations were performed independently several times, with consistent results.

to cisplatin (measured as viability after 72 hours in different concentrations of cisplatin; Figure 6A). The cultures were harvested or assayed immediately on growing back to 80% confluence, and a modest reduction in total NUP62 was detected by using Western blot analysis of the cultures after one or two cycles of selection (Figure 6B). We also queried whether knockdown of NUP62 confers extended resistance to cisplatin independently of exposure to the drug. Cells were treated with NUP62 or control siRNA for 72 hours, siRNA was removed from the medium, the cells were cultured for nine generations (three passes of 1:8), and then the cells were tested for sensitivity to cisplatin. Surprisingly, in the absence of prior exposure to cisplatin and after sufficient culture time to dilute parent (siRNA-treated) cells to at least 1:512, a modest, but statistically significant, level of cisplatin resistance was detected (Figure 6C). Western blot analyses did not reveal an obvious difference in total NUP62 accumulation between control and NUP62 siRNA-treated cultures after nine generations, although it is possible that moderate changes in a fraction of the cells or changes restricted to a short phase of the cell cycle would escape detection by this gross method.

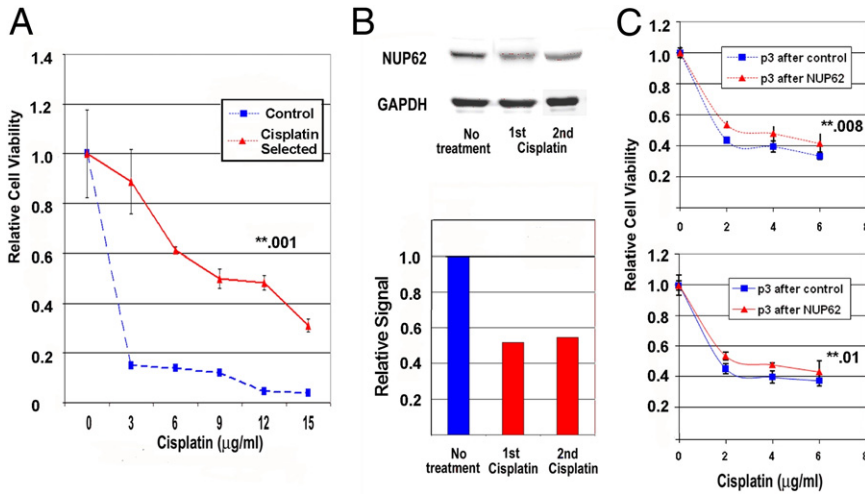


Figure 6. Cisplatin-selected TOV112D cells display modest reduction of NUP62; cells treated with NUP62 siRNA retain some cisplatin resistance after several generations. **A:** TOV112D-9 cells were selected by two rounds of treatment with 4 µg/mL cisplatin for 48 hours and recovery, and analyzed for relative viability after treatment with different concentrations of cisplatin for 72 hours. Cells from the first passage after recovery were analyzed. **B:** **Top panel:** Western blot analysis of TOV112D-9 cells after one or two rounds of treatment and recovery from 4 µg/mL cisplatin for 48 hours. **Bottom panel:** Relative band densities normalized to GAPDH. Cells from the first passage after recovery were analyzed. **C:** Pretreatment of TOV112D TOV112D-CAP (**bottom**) cells with NUP62 siRNA for 72 hours confers resistance to cisplatin that is partly retained over several generations. **Top and bottom:** Independent experiments. After treatment with NUP62 siRNA, the cells were cultured for three passes of 1:8, then tested for sensitivity to different concentrations of cisplatin treatment for 48 hours. The results are shown with paired *t*-test *P* values.

Induction and Release of Tumor Cells from Dormancy by Modulation of NUP62 Expression

As previously indicated, knockdown of NUP62 results in growth arrest that is reversible on removal of NUP62 siRNA, whereas knockdown of NUP62 and treatment with cisplatin result in enhancement of survival, accompanied by entry of cells into protracted growth arrest (dormancy). We sought to determine whether induction of NUP62 expression awakened the latter cells from dormancy. The TOV112D-9 (containing only pTet-on) and TOV112D-CAP (containing both pTet-on and TRE-NUP62) cell lines cultured in tetracycline-free medium were treated on day 1 with NUP62 or control siRNA for 24 hours; then, 4.5 µg/mL cisplatin was added to some cultures for 72 hours (+Cis, day 5; Figure 7, A and B). Cisplatin and siRNAs were removed, and the cells were cultured in nominal medium for 7 days (+Cis, day 12; Figure 7, A and B). Doxycycline was added to some cultures for 5 days and then removed, and the cultures were maintained in nominal medium for 7 additional days (+Cis, +Dox, day 24; Figure 7B). For the TOV112D-9 cells, the cultures were also maintained for a further 6 weeks, with changes of nominal medium every 4 days (+Cis, +Dox, day 66; Figure 7B). As shown in Figure 7B, TOV112D-9 cells at day 24 displayed no colonies. Rarely, a few colonies will appear in the TOV112D-9 cultures treated with NUP62 siRNA and cisplatin after being maintained for ≥6 weeks, such as the two small colonies appearing at day 66 (Figure 7B). In contrast, TOV112D-CAP cells treated with NUP62 siRNA and cisplatin displayed abundant colonial growth soon after transient treatment with doxycycline (+Cis, +Dox, day 24; Figure 7B), but only a few large colonies were present in parallel cultures that were not treated with doxycycline (+Cis, -Dox, day 24; Figure 7B). In TOV112D-CAP cultures that were treated with NUP62 siRNA and cisplatin, two types of colonies could be distinguished at day 24 after treatment with doxycycline: sparse large colonies and abundant small colonies. In similarly treated TOV112D-CAP cultures lacking doxycycline, only sparse large colonies were observed at day 24.

We interpret the data from the colony assays as follows: TOV112D-9 cultures lack the doxycycline-inducible NUP62 expression construct, and, thus, only express NUP62 from the endogenous gene. On knock-

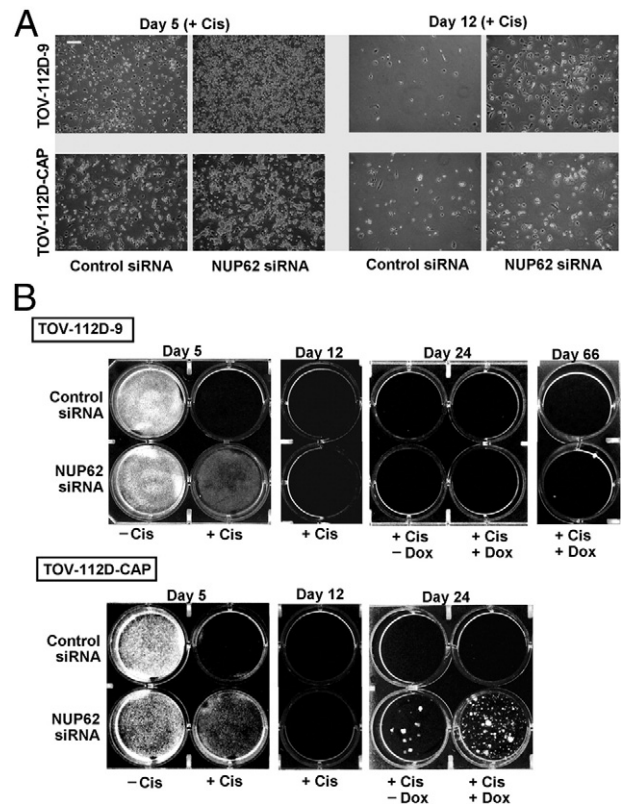


Figure 7. Entry or exit of TOV112D cells from drug-resistant dormancy can be induced by modulation of NUP62 expression. TOV112D-9 or TOV112D-CAP cells were grown to 80% confluence (day 0), treated with control or NUP62 siRNA for 24 hours (day 1), then cultured for 3 days in the absence (-Cis) or presence (+Cis) of cisplatin (day 5). Cisplatin and siRNAs were removed on day 5, and the cells were cultured for 7 days (day 12). Doxycycline was added to some of the cultures for 5 days (+Dox), then removed, and the cultures were maintained for 7 more days (day 24). The TOV112D cells were also maintained for 6 weeks longer in the absence of cisplatin and siRNAs (day 66). **A:** Phase-contrast microscopy of cultures at days 5 and 12. Scale bar = 100 µm. **B:** Cultures were fixed and stained with crystal violet. Reverse black-and-white images are shown for clarity.

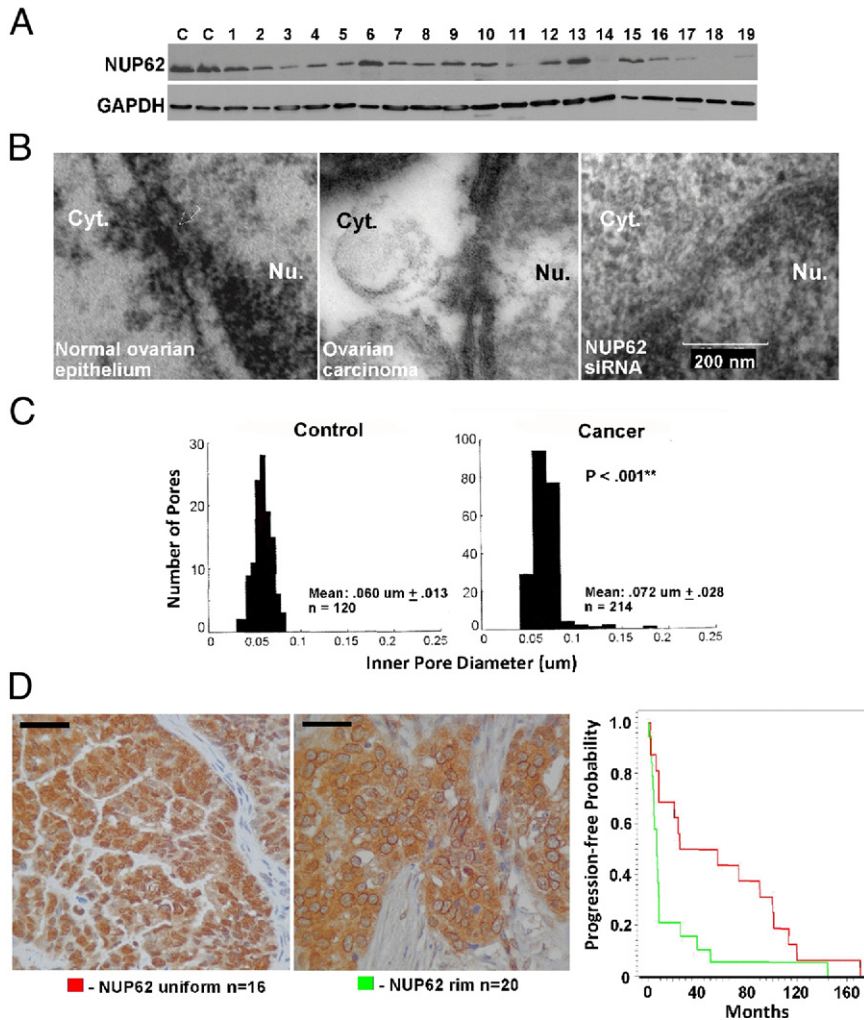


Figure 8. Alterations in NUP62 accumulation and distribution in high-grade ovarian carcinomas. **A:** From whole tissue, homogenates of fresh resected primary and metastatic high-grade serous ovarian carcinomas were analyzed using Western blot analysis for NUP62 accumulation (equal total protein per lane). Normal ovarian tissue was derived from epithelial cell–dense gyri on the surface of the ovary. **B:** Transmission electron microscopy of an NPC in normal ovarian epithelium [which contains a dense inner ring (arrow)], in high-grade serous ovarian carcinoma, and in TOV112D cells treated with NUP62 siRNA. Cytoplasmic (Cyt.) and nuclear (Nu.) compartments are indicated. **C:** Measurement and comparison of inner pore diameters of NPCs from four high-grade serous ovarian carcinomas with four normal ovarian epithelium samples. **D:** IHC stains of paraffin-embedded, high-grade ovarian serous carcinoma sections distinguished two patterns of staining that appeared in various proportions among cells in each tumor. **Left panel:** Red, a tumor with a high portion of uniform staining across the entire nucleus. **Center panel:** Green, a tumor with a high portion of defined perimetrical staining around the nucleus, with little staining in the central region. **Right panel:** Samples were scored and counted for perimetrical and uniform NUP62 nuclear staining; tumors displaying a greater fraction of perimetrical stained tumor nuclei (green type) were distinguished from those displaying a greater fraction of uniform nuclear staining (red type). A Kaplan-Meier analysis of the progression-free interval for these two populations is shown.

down of NUP62, cisplatin treatment, and removal of cisplatin, the resistant TOV112D-9 cells enter dormancy, interrupted in long-term cultures only by the rare stochastic conversion to growth of single cells, leading to the formation of a colony. After knockdown of NUP62, treatment with cisplatin, and removal of cisplatin, TOV112D-CAP cells also enter dormancy but are pushed back into the cell cycle when expression of NUP62 is induced by transient treatment with doxycycline. This is apparent from an abundance of small colonies that appear after treatment of TOV112D-CAP cultures with doxycycline. The sparse large colonies that appear in TOV112D-CAP but not TOV112D-9 cultures have a related ontogeny. Although the tetracycline transactivator protein is engineered to bind and activate the TRE when associated with doxycycline, a low level of binding is present in the absence of doxycycline, and incrementally higher levels of NUP62 expression probably arise in some cells. After removal of cisplatin, the emergence of these cells precedes that of the TOV112D-CAP cells that are stimulated to growth by doxycycline and results in the generation of a few large colonies in both cultures with and without doxycycline.

Variation of NUP62 Accumulation and Distribution in Ovarian Carcinomas

To begin to explore whether modulation of NUP62 accumulation and NPC architecture occur during tumor growth *in vivo*, tissue homogenates from primary and metastatic high-grade ovarian carcinomas (fresh resected tumors) were analyzed by using Western blot analysis for NUP62 accumulation. A comparison of the relative intensities of the NUP62 bands indicated that many ovarian carcinomas accumulate less total NUP62 than normal ovarian tissue (derived from epithelial cell–dense gyri on the surface of the ovary; Figure 8A). Furthermore, the nuclear pore structure of normal ovarian epithelial and ovarian serous carcinoma cells was observed by transmission electron microscopy. Embedded in the central channel of the nuclear pore of normal ovarian epithelial cells is an electron-dense bar of material that represents the two inner ring structures containing the NUP62 complex. The central channel of nuclear pores in ovarian epithelial tumor cells frequently lacked this electron-dense bar, as did nuclear pores from cultured tumor cells treated with NUP62 siRNA (Figure 8B). The absence of

this material gave the nuclear pores of some tumor cells a dilated appearance, as was quantified by comparison of the inner pore diameters from four ovarian carcinomas (high-grade serous) with those from the ovarian surface epithelia of four healthy controls (Figure 8C). Interestingly, the frequent appearance of dilated nuclear pores in ovarian carcinoma cells is similar to the appearance of nuclear pores in picornavirus infected cells, consistent with the observation that picornavirus infection also results in down-regulation of NUP62.⁵⁸

Because NUP62 is distributed between NPC and intranuclear and cytoplasmic pools, distribution of NUP62 among these pools and among NPC populations may relate to tumor phenotype. Although differences in total accumulation of NUP62 may affect drug resistance and/or dormancy, redistribution of NUP62 between nuclear and cytoplasmic pools, or between NPC populations, may be functionally equivalent. Although immunohistochemical (IHC) studies have limited resolution at the subcellular level, it is nonetheless possible to distinguish grossly different nuclear and cytoplasmic distributions of NUP62. By using IHC stains of paraffin-embedded tissue sections, we distinguished two general distributions of NUP62 in the nuclei of high-grade ovarian carcinomas: a relatively uniform dense staining across the entire nucleus and a discrete perimetrical ring of staining on the nuclear envelope, with little staining in the central regions (Figure 8D). One interpretation of these staining patterns is that the tight perimetrical pattern represents an attenuated NUP62 distribution that is restricted to a dense ring of NPCs on the nuclear envelope, whereas the uniform pattern represents cells with more abundant NUP62 distributed among NPCs at additional sites on the entire nuclear envelope, and possibly in intranuclear sites as well. We evaluated the utility of these two NPC patterns with a training group of pathological specimens from patients with stage III ovarian carcinomas subsequently given primary platinum therapy and observed. The samples were scored and counted for perimetrical and uniform NUP62 nuclear staining. Tumors displaying a greater fraction of perimetrical stained tumor nuclei were distinguished from those displaying greater uniform nuclear staining. As shown in Figure 8D, Kaplan-Meier analysis of the progression-free interval indicated that increased frequency of perimetrical rim NUP62 staining nuclei in a tumor may predict a poor response to platinum chemotherapy (log-rank *P* value, 0.018; Wilcoxon *P* value, 0.016).

Discussion

Inhibition of G₁ or G₂ phase cell cycle progression by most cytostatic agents has enhanced, rather than reduced, the cytotoxicity of cisplatin.^{42–48} Thus, although knockdown of NUP62 results in cell cycle arrest, protection against cisplatin cannot result merely from restricting progression of cells into or through the S phase. Rather, cisplatin resistance after knockdown of NUP62 may be conferred by protective or anti-apoptotic mechanisms that are restricted to the specific stage of the G₁ phase of the cell cycle, in which the cells are paused. By compar-

ison with cell cycle arrest in aphidicolin-treated cells, we showed that knockdown of NUP62 results in a pause in cell cycle progression at a point upstream from the G₁-S border. Interestingly, cells that pass this point appear competent to complete the remainder of the cell cycle, even in the continuing presence of NUP62 siRNA, suggesting that NUP62 knockdown blocks progression exclusively through this stage of the G₁ phase. Western blot analyses revealed that total NUP62 accumulation displays a peak early in the G₁ phase, before the peak of cyclin E accumulation. Together, the data suggest that enhanced accumulation of NUP62 may be required for passage through an early stage of the G₁ phase. The relationship of this G₁ phase restriction point to other restriction points in the G₁ phase, including those directed by phosphatidylinositol 3-kinase, contact inhibition or growth factor depletion, and/or differentiation,⁵⁹ remains to be investigated. Whether a specific restriction point exists in the early G₁ phase that can only be passed if a critical number or fraction of NUP62⁺ NPCs has been achieved remains to be further elucidated. In contrast to knockdown, overexpression of NUP62 resulted in apoptosis, depleting cells from the G₁ phase in asynchronous cultures. This observation suggests that both up- and down-regulation of NUP62 during the G₁ phase may be required for successful transit of cells to the S phase.

Although the observed pause in the G₁ phase after NUP62 knockdown may be functionally related to entry of TOV112D-9 and TOV112D-CAP cells into dormancy, cisplatin resistance could be conferred by cell cycle-independent effects of increasing the abundance of NUP62-depleted NPCs. The NUP62 content of NPCs could influence sensitivity to cisplatin through several possible mechanisms; however, reduction of nucleocytoplasmic transport mediated by NUP62 does not appear to be one of them. Knockdown of NUP160, which dismantles the NPC, or of both NUP62 and NUP160 did not detectably reduce TOV112D-9 cell sensitivity to the cytotoxic effect of cisplatin, suggesting that mere disruption of nucleocytoplasmic transport does not confer resistance. Rather, the enrichment of NUP62-depleted NPC complexes appears to confer cisplatin resistance through an active mechanism. In addition to nucleocytoplasmic transport, the NPC functions in the organization of underlying chromatin, and NUPs appear to function in transcriptional regulation and in the intranuclear movement of certain genes from transcriptionally silent, heterochromatic peripheral regions of the nucleus to transcriptionally active, euchromatic central regions.^{36,37,60,61} The enrichment of NUP62-depleted NPC complexes may directly affect the organization of underlying chromatin and, thereby, reduce sensitivity to cisplatin by altering gene expression or by other potential mechanisms, including limiting access of the drug to certain regions of DNA.

Treatment of TOV112D-9 cells with NUP62 siRNA results in growth retardation, but normal growth resumes within a few days after removal of siRNA. In contrast, treatment with NUP62 siRNA and cisplatin resulted in the surviving cells entering a state of growth arrest that was refractory to removal of NUP62 siRNA and cisplatin. It is possible that treatment with NUP62 siRNA alone pro-

duces two populations of cells, one that is in transient growth arrest and a smaller population that has entered dormancy, with the latter population resistant to cisplatin. Thus, in the absence of cisplatin selection, removal of NUP62 siRNA would permit regrowth of the population in transient growth arrest over the dormant population. After cisplatin selection, only the dormant population would remain, and this population would not grow back spontaneously after removal of NUP62 siRNA. The delay in recovery of proliferating cultures after removal of NUP62 siRNA is consistent with this model, although that delay may be merely the time required for *de novo* expression and translation of NUP62. Also, cultures treated with NUP62 siRNA in the absence of cisplatin retain some cisplatin resistance after several generations, supporting the view that resistant cells have the capacity to proliferate after the removal of NUP62 siRNA. The retention of cisplatin resistance several cell generations after the removal of NUP62 siRNA also suggests that knockdown of NUP62 confers changes to chromatin organization that are somehow retained during proliferation. Such changes may represent a novel pathway for epigenetic regulation.

At least three major mechanisms have been associated with tumor dormancy: generation of tumor vasculature (angiogenesis), evasion of immune responses, and entry/exit of tumor cells from the cell cycle (sometimes distinguished as cellular dormancy^{49,62}). Tumor dormancy can follow therapeutic intervention, but it is also exhibited by primary tumors, because their growth can lag or stall before they become clinically significant.^{63–65} Protracted tumor dormancy can occur after treatment; tumor cells that resist therapy can persist in an occult or asymptomatic state for years before causing a recurrence of disease.⁶⁶ The mechanisms of cancer cell relevation to cellular dormancy, whether preceded by therapeutic intervention or during progression to an oncogenic state, are not well understood. The mechanisms that induce dormant cancer cells to awaken and proliferate are equally elusive. The culture system presented herein offers a controlled platform from which to study entry of tumor cells into protracted quiescence after treatment with a therapeutic agent, as well as a rapid mechanism for awakening dormant cells and inducing proliferation. Some evidence is presented herein that intrinsic modulation of NUP62 may be a direct mechanism through which ovarian carcinomas resist therapeutics and/or enter or exit from cellular dormancy. It is not clear the synthetic level at which accumulation of NUP62 is regulated, and whether changes in NPC architecture arise exclusively from changes in NUP62 accumulation or from other mechanisms, such as subcellular redistribution. Changes in NPC architecture and/or the associated changes in chromatin organization may be effectors of drug resistance or dormancy; they also may lie downstream from other signaling pathways or regulators. Modulation of NUP62 represents a method to produce relatively uniform populations of cells either entering or exiting protracted dormancy and drug resistance, and gene expression profiling and bioinformatic techniques can be applied to this system to yield further insights into

the signaling and effector systems that affect these processes.

The defective state of p53 in TOV112D cells indicates that induction of drug resistance and/or dormancy by NUP62 knockdown does not require p53. Many studies^{67–69} have demonstrated a central role for p53 in directing tumor cells toward premature senescence, and recently, removal of senescent tumor cells by the immune system has been identified as a mechanism of tumor clearance.⁷⁰ Senescence and tumor cell dormancy, although both quiescent states (albeit one terminal and the other not), may differ by a stronger relationship between dormant cells and cancer stem cells, the pool of cells involved in tumor renewal. Although loss of p53 function may be a key mechanism through which epithelial tumor cells escape senescence, and p53 activity may maintain angiogenesis-restricted dormancy,^{71–73} a connection between p53 activity and entry or exit from cellular dormancy has not been established. In fact, recent studies⁷⁴ have suggested an oppositional relationship between p53 activity and expansion of the stem cell phenotype. In the experiments presented herein, the TOV112D cells are derived from a high-grade ovarian epithelial carcinoma with endometrioid histological features, and they express defective p53.³⁸ An interesting query for future studies will be how the effects of NUP62 knockdown on drug resistance and dormancy compare in tumor cell lines with normal or defective p53.

The pro-apoptotic effect of NUP62 overexpression may be reminiscent of p53: activation of p53 restricts cell cycle progression at both the late G₁ phase and G₂-M,⁷⁵ whereas NUP62 knockdown restricts progression only through a part of the G₁ phase. Alterations in the p53 gene have been associated with variable responses to cisplatin in cultured cell lines, including some lines derived from ovarian tumors.^{10,76} Further study has shown that, although p53 activation may contribute to the cytotoxic response to cisplatin of normal cells, such as kidney epithelium,^{77,78} the role of p53 status in the relative responses of ovarian epithelial tumors is not as clear.^{79,80} Because tumor cells with defective p53 can display sensitivity to cisplatin, it is apparent that the response to cisplatin in tumor cells may use alternate pathways.^{81–83} Equally important, p53 defects are prevalent in high-grade ovarian epithelial tumors and in some other epithelial tumor types, suggesting that these mutations occur early during the tumorigenic progression of these cancer cell lineages.^{18,19} Prognostic breakdown of high-grade cancers using gene expression profiling approaches, however, has proved challenging.^{84,85} The results presented herein suggest that a better understanding of the three-dimensional structure of the nucleus, in particular the spatial arrangement and architecture of the NPCs and the underlying effects on chromatin organization, could provide insights into predicting how different high-grade ovarian carcinomas will respond to therapeutic intervention.

Epigenetic regulatory mechanisms can work in concert with somatic mutations to drive tumor progression and promote tumor cell survival. For example, in a subset of ovarian carcinomas (perhaps as high as 20%), methyl-

ation of FANCF or BRCA1 generates genomic instability, thereby promoting other neoplastic changes.⁸⁶ Subsequent reversion of these genes to demethylated forms restores drug tolerance to this subset of cancers. The epigenetic machinery of the cell includes DNA methylation, histone modifications, noncoding RNAs, and chromatin remodeling and organization, the latter being affected by the first three and by the architecture of the nucleus. In addition, contingent on gene and tissue type,^{61,87} metazoan genes localized adjacent to the nuclear envelope generally tend to be suppressed, whereas genes localized centrally in the nucleoplasm tend to be transcriptionally active.^{60,88} Chromatin organization appears to be influenced by its proximity to the NPC, because channels of euchromatin interrupt the lamina and extend from the NPC into the nucleus.⁸⁹ Although associations between specific NPCs and specific gene groups have not yet been reported in metazoans, studies^{90,91} in *Drosophila* and human fibroblasts have shown that chromosomal organization in the interphase nucleus is directed by specific associations between chromatin and the nuclear lamina. Future studies could be aimed at how changes in NPC architecture affect chromatin organization directly or indirectly through interactions with the nuclear lamina. The outcome of such studies may better define how changes in NUP abundance or in NPC architecture influence gene expression and how such mechanisms contribute to the phenotypic diversity and adaptive responses of cancer cells.

References

- Jemal A, Siegel R, Ward E, Hao Y, Xu J, Thun MJ: Cancer statistics, 2009. *CA Cancer J Clin* 2009, 59:225–249
- Borst P, Rottenberg S, Jonkers J: How do real tumors become resistant to cisplatin? *Cell Cycle* 2008, 7:1353–1359
- Knipp M: Metallothioneins and platinum(II) anti-tumor compounds. *Curr Med Chem* 2009, 16:522–537
- Noel EE, Yeste-Velasco M, Mao X, Perry J, Kudahetti SC, Li NF, Sharp S, Chaplin T, Xue L, McIntyre A, Shan L, Powles T, Oliver RT, Young BD, Shipley J, Berney DM, Joel SP, Lu YJ: The association of CCND1 overexpression and cisplatin resistance in testicular germ cell tumors and other cancers. *Am J Pathol* 2010, 2010:15
- Codegani AM, Broggin M, Pitelli MR, Pantarotto M, Torri V, Mangioni C, D'Incalci M: Expression of genes of potential importance in the response to chemotherapy and DNA repair in patients with ovarian cancer. *Gynecol Oncol* 1997, 65:130–137
- Selvakumaran M, Pisarcik DA, Bao R, Yeung AT, Hamilton TC: Enhanced cisplatin cytotoxicity by disturbing the nucleotide excision repair pathway in ovarian cancer cell lines. *Cancer Res* 2003, 63:1311–1316
- Townsend DM, Findlay VL, Tew KD: Glutathione S-transferases as regulators of kinase pathways and anticancer drug targets. *Methods Enzymol* 2005, 401:287–307
- Wang Y, Niu XL, Qu Y, Wu J, Zhu YQ, Sun WJ, Li LZ: Autocrine production of interleukin-6 confers cisplatin and paclitaxel resistance in ovarian cancer cells. *Cancer Lett* 2010, 2010:14
- Sherman-Baust CA, Weeraratna AT, Rangel LB, Pizer ES, Cho KR, Schwartz DR, Shock T, Morin PJ: Remodeling of the extracellular matrix through overexpression of collagen VI contributes to cisplatin resistance in ovarian cancer cells. *Cancer Cell* 2003, 3:377–386
- Perego P, Giarola M, Righetti SC, Supino R, Caserini C, Delia D, Pierotti MA, Miyashita T, Reed JC, Zunino F: Association between cisplatin resistance and mutation of p53 gene and reduced bax expression in ovarian carcinoma cell systems. *Cancer Res* 1996, 56:556–562
- Wang X, Liu Y, Chow LS, Wong SC, Tsao SW, Kwong DL, Wang J, Sham JS, Nicholls JM: Cisplatin-induced p53-independent growth arrest and cell death in cancer cells. *Int J Oncol* 1999, 15:1097–1102
- Schuijjer M, Berns EM: TP53 and ovarian cancer. *Hum Mutat* 2003, 21:285–291
- Mansouri A, Zhang Q, Ridgway LD, Tian L, Claret FX: Cisplatin resistance in an ovarian carcinoma is associated with a defect in programmed cell death control through XIAP regulation. *Oncol Res* 2003, 13:399–404
- Ma JJ, Chen BL, Xin XY: XIAP gene downregulation by small interfering RNA inhibits proliferation, induces apoptosis, and reverses the cisplatin resistance of ovarian carcinoma. *Eur J Obstet Gynecol Reprod Biol* 2009, 146:222–226
- Asselin E, Mills GB, Tsang BK: XIAP regulates Akt activity and caspase-3-dependent cleavage during cisplatin-induced apoptosis in human ovarian epithelial cancer cells. *Cancer Res* 2001, 61:1862–1868
- Yang X, Fraser M, Abedini MR, Bai T, Tsang BK: Regulation of apoptosis-inducing factor-mediated, cisplatin-induced apoptosis by Akt. *Br J Cancer* 2008, 98:803–808
- Abedini MR, Muller EJ, Bergeron R, Gray DA, Tsang BK: Akt promotes chemoresistance in human ovarian cancer cells by modulating cisplatin-induced, p53-dependent ubiquitination of FLICE-like inhibitory protein. *Oncogene* 2009, 29:11–25
- Salani R, Kurman RJ, Giuntoli R 2nd, Gardner G, Bristow R, Wang TL, Shih IM: Assessment of TP53 mutation using purified tissue samples of ovarian serous carcinomas reveals a higher mutation rate than previously reported and does not correlate with drug resistance. *Int J Gynecol Cancer* 2008, 18:487–491
- Ahmed AA, Etemadmoghadam D, Temple J, Lynch AG, Riad M, Sharma R, Stewart C, Fereday S, Caldas C, Defazio A, Bowtell D, Brenton JD: Driver mutations in TP53 are ubiquitous in high grade serous carcinoma of the ovary. *J Pathol* 2010, 221:49–56
- Cara S, Tannock IF: Retreatment of patients with the same chemotherapy: implications for clinical mechanisms of drug resistance. *Ann Oncol* 2001, 12:23–27
- Seltzer V, Vogl S, Kaplan B: Recurrent ovarian carcinoma: retreatment utilizing combination chemotherapy including cis-diamminedichloroplatinum in patients previously responding to this agent. *Gynecol Oncol* 1985, 21:167–176
- Rottenberg S, Nygren AO, Pajic M, van Leeuwen FW, van der Heijden I, van de Wetering K, Liu X, de Visser KE, Gilhuijs KG, van Tellingen O, Schouten JP, Jonkers J, Borst P: Selective induction of chemotherapy resistance of mammary tumors in a conditional mouse model for hereditary breast cancer. *Proc Natl Acad Sci U S A* 2007, 104:12117–12122
- Sharma SV, Lee DY, Li B, Quinlan MP, Takahashi F, Maheswaran S, McDermott U, Azizian N, Zou L, Fischbach MA, Wong KK, Brandstetter K, Wittner B, Ramaswamy S, Classon M, Settleman J: A chromatin-mediated reversible drug-tolerant state in cancer cell subpopulations. *Cell* 2010, 141:69–80
- Beck M, Forster F, Ecke M, Plitzko JM, Melchior F, Gerisch G, Baumeister W, Medalia O: Nuclear pore complex structure and dynamics revealed by cryoelectron tomography. *Science* 2004, 306:1387–1390
- Alber F, Dokudovskaya S, Veenhoff LM, Zhang W, Kipper J, Devos D, Suprpto A, Karni-Schmidt O, Williams R, Chait BT, Sali A, Rout MP: The molecular architecture of the nuclear pore complex. *Nature* 2007, 450:695–701
- Lim RY, Fahrenkrog B: The nuclear pore complex up close. *Curr Opin Cell Biol* 2006, 18:342–347
- Boer JM, van Deursen JM, Croes HJ, Fransen JA, Grosveld GC: The nucleoporin CAN/Nup214 binds to both the cytoplasmic and the nucleoplasmic sides of the nuclear pore complex in overexpressing cells. *Exp Cell Res* 1997, 232:182–185
- Bastos R, Ribas de Pouplana L, Enarson M, Bodoor K, Burke B: Nup84, a novel nucleoporin that is associated with CAN/Nup214 on the cytoplasmic face of the nuclear pore complex. *J Cell Biol* 1997, 137:989–1000
- Fahrenkrog B, Maco B, Fager AM, Koser J, Sauder U, Ullman KS, Aebi U: Domain-specific antibodies reveal multiple-site topology of Nup153 within the nuclear pore complex. *J Struct Biol* 2002, 140:254–267

30. Hutten S, Walde S, Spillner C, Hauber J, Kehlenbach RH: The nuclear pore component Nup358 promotes transportin-dependent nuclear import. *J Cell Sci* 2009, 122:1100–1110
31. Hu T, Guan T, Gerace L: Molecular and functional characterization of the p62 complex, an assembly of nuclear pore complex glycoproteins. *J Cell Biol* 1996, 134:589–601
32. Guan T, Muller S, Klier G, Pante N, Blevitt JM, Haner M, Paschal B, Aebi U, Gerace L: Structural analysis of the p62 complex, an assembly of O-linked glycoproteins that localizes near the central gated channel of the nuclear pore complex. *Mol Biol Cell* 1995, 6:1591–1603
33. Griffis ER, Xu S, Powers MA: Nup98 localizes to both nuclear and cytoplasmic sides of the nuclear pore and binds to two distinct nucleoporin subcomplexes. *Mol Biol Cell* 2003, 14:600–610
34. Terry LJ, Wentz SR: Flexible gates: dynamic topologies and functions for FG nucleoporins in nucleocytoplasmic transport. *Eukaryot Cell* 2009, 8:1814–1827
35. Capelson M, Liang Y, Schulte R, Mair W, Wagner U, Hetzer MW: Chromatin-bound nuclear pore components regulate gene expression in higher eukaryotes. *Cell* 2010, 140:372–383
36. Kalverda B, Pickersgill H, Shloma VV, Fornerod M: Nucleoporins directly stimulate expression of developmental and cell-cycle genes inside the nucleoplasm. *Cell* 2010, 140:360–371
37. Kalverda B, Fornerod M: The nuclear life of nucleoporins. *Dev Cell* 2007, 13:164–165
38. Provencher DM, Lounis H, Champoux L, Tetrault M, Manderson EN, Wang JC, Eydoux P, Savoie R, Tonin PN, Mes-Masson AM: Characterization of four novel epithelial ovarian cancer cell lines. *In Vitro Cell Dev Biol Anim* 2000, 36:357–361
39. Singer G, Stohr R, Cope L, Dehari R, Hartmann A, Cao DF, Wang TL, Kurman RJ, Shih le M: Patterns of p53 mutations separate ovarian serous borderline tumors and low- and high-grade carcinomas and provide support for a new model of ovarian carcinogenesis: a mutational analysis with immunohistochemical correlation. *Am J Surg Pathol* 2005, 29:218–224
40. Vang R, Shih le M, Kurman RJ: Ovarian low-grade and high-grade serous carcinoma: pathogenesis, clinicopathologic and molecular biologic features, and diagnostic problems. *Adv Anat Pathol* 2009, 16:267–282
41. Roh MH, Yassin Y, Miron A, Mehra KK, Mehrad M, Monte NM, Mutter GL, Nucci MR, Ning G, McKeon FD, Hirsch MS, Wa X, Crum CP: High-grade fimbrial-ovarian carcinomas are unified by altered p53, PTEN and PAX2 expression. *Mod Pathol* 2010, 23:1316–1324
42. Lincet H, Poulain L, Remy JS, Deslandes E, Duigou F, Gauduchon P, Staedel C: The p21(cip1/waf1) cyclin-dependent kinase inhibitor enhances the cytotoxic effect of cisplatin in human ovarian carcinoma cells. *Cancer Lett* 2000, 161:17–26
43. Deng X, Kim M, Vandier D, Jung YJ, Rikiyama T, Sgagias MK, Goldsmith M, Cowan KH: Recombinant adenovirus-mediated p14(ARF) overexpression sensitizes human breast cancer cells to cisplatin. *Biochem Biophys Res Commun* 2002, 296:792–798
44. Smalley KS, Eisen TG: Farnesyl transferase inhibitor SCH66336 is cytostatic, pro-apoptotic and enhances chemosensitivity to cisplatin in melanoma cells. *Int J Cancer* 2003, 105:165–175
45. Coley HM, Shotton CF, Kokkinos MI, Thomas H: The effects of the CDK inhibitor seliciclib alone or in combination with cisplatin in human uterine sarcoma cell lines. *Gynecol Oncol* 2007, 105:462–469
46. Vlachos P, Nyman U, Hajji N, Joseph B: The cell cycle inhibitor p57(Kip2) promotes cell death via the mitochondrial apoptotic pathway. *Cell Death Differ* 2007, 14:1497–1507
47. Bu Y, Lu C, Bian C, Wang J, Li J, Zhang B, Li Z, Brewer G, Zhao RC: Knockdown of Dicer in MCF-7 human breast carcinoma cells results in G1 arrest and increased sensitivity to cisplatin. *Oncol Rep* 2009, 21:13–17
48. Singh RK, Lange TS, Kim KK, Brard L: A coumarin derivative (RKS262) inhibits cell-cycle progression, causes pro-apoptotic signaling and cytotoxicity in ovarian cancer cells. *Invest New Drugs* 2009, 29:29
49. Aguirre-Ghiso JA: Models, mechanisms and clinical evidence for cancer dormancy. *Nat Rev Cancer* 2007, 7:834–846
50. Maeshima K, Yahata K, Sasaki Y, Nakatomi R, Tachibana T, Hashikawa T, Imamoto F, Imamoto N: Cell-cycle-dependent dynamics of nuclear pores: pore-free islands and lamins. *J Cell Sci* 2006, 119:4442–4451
51. Kinoshita Y, Johnson EM: Site-specific loading of an MCM protein complex in a DNA replication initiation zone upstream of the c-MYC gene in the HeLa cell cycle. *J Biol Chem* 2004, 279:35879–35889
52. Meier E, Miller BR, Forbes DJ: Nuclear pore complex assembly studied with a biochemical assay for annulate lamellae formation. *J Cell Biol* 1995, 129:1459–1472
53. Ewald A, Kossner U, Scheer U, Dabauvalle MC: A biochemical and immunological comparison of nuclear and cytoplasmic pore complexes. *J Cell Sci* 1996, 109(Pt 7):1813–1824
54. Walther TC, Alves A, Pickersgill H, Loiodice I, Hetzer M, Galy V, Hulsmann BB, Kocher T, Wilm M, Allen T, Mattaj JW, Doye V: The conserved Nup107-160 complex is critical for nuclear pore complex assembly. *Cell* 2003, 113:195–206
55. Davis LI, Blobel G: Nuclear pore complex contains a family of glycoproteins that includes p62: glycosylation through a previously unidentified cellular pathway. *Proc Natl Acad Sci U S A* 1987, 84:7552–7556
56. Paulson JR, Taylor SS: Phosphorylation of histones 1 and 3 and nonhistone high mobility group 14 by an endogenous kinase in HeLa metaphase chromosomes. *J Biol Chem* 1982, 257:6064–6072
57. Bloom J, Cross FR: Multiple levels of cyclin specificity in cell-cycle control. *Nat Rev Mol Cell Biol* 2007, 8:149–160
58. Belov GA, Lidsky PV, Mikitas OV, Egger D, Lukyanov KA, Bienz K, Agol VI: Bidirectional increase in permeability of nuclear envelope upon poliovirus infection and accompanying alterations of nuclear pores. *J Virol* 2004, 78:10166–10177
59. Hulleman E, Boonstra J: Regulation of G1 phase progression by growth factors and the extracellular matrix. *Cell Mol Life Sci* 2001, 58:80–93
60. Malik P, Zuleger N, Schirmer EC: Nuclear envelope influences on genome organization. *Biochem Soc Trans* 2010, 38:268–272
61. Meister P, Towbin BD, Pike BL, Ponti A, Gasser SM: The spatial dynamics of tissue-specific promoters during *C. elegans* development. *Genes Dev* 2010, 24:766–782
62. Almog N: Molecular mechanisms underlying tumor dormancy. *Cancer Lett* 2010, 294:139–146
63. Harach HR, Franssila KO, Wasenius VM: Occult papillary carcinoma of the thyroid: a "normal" finding in Finland A systematic autopsy study. *Cancer* 1985, 56:531–538
64. Nielsen M, Thomsen JL, Primdahl S, Dyreborg U, Andersen JA: Breast cancer and atypia among young and middle-aged women: a study of 110 medicolegal autopsies. *Br J Cancer* 1987, 56:814–819
65. Black WC, Welch HG: Advances in diagnostic imaging and overestimations of disease prevalence and the benefits of therapy. *N Engl J Med* 1993, 328:1237–1243
66. Udagawa T: Tumor dormancy of primary and secondary cancers. *Apms* 2008, 116:615–628
67. Zilfou JT, Lowe SW: Tumor suppressive functions of p53. *Cold Spring Harb Perspect Biol* 2009, 1:a001883
68. Zuckerman V, Wolyniec K, Sionov RV, Haupt S, Haupt Y: Tumour suppression by p53: the importance of apoptosis and cellular senescence. *J Pathol* 2009, 219:3–15
69. McDuff FK, Turner SD: Jailbreak: oncogene-induced senescence and its evasion. *Cell Signal* 2011, 23:6–13
70. Xue W, Zender L, Miething C, Dickins RA, Hernando E, Krizhanovsky V, Cordon-Cardo C, Lowe SW: Senescence and tumour clearance is triggered by p53 restoration in murine liver carcinomas. *Nature* 2007, 445:656–660
71. Holmgren L, O'Reilly MS, Folkman J: Dormancy of micrometastases: balanced proliferation and apoptosis in the presence of angiogenesis suppression. *Nat Med* 1995, 1:149–153
72. Holmgren L, Jackson G, Arbiser J: p53 Induces angiogenesis-restricted dormancy in a mouse fibrosarcoma. *Oncogene* 1998, 17:819–824
73. Nagayama Y, Shigematsu K, Namba H, Zeki K, Yamashita S, Niwa M: Inhibition of angiogenesis and tumorigenesis, and induction of dormancy by p53 in a p53-null thyroid carcinoma cell line in vivo. *Anticancer Res* 2000, 20:2723–2728
74. Mehta S, Huillard E, Kesari S, Maire CL, Golebiowski D, Harrington EP, Alberta JA, Kane MF, Theisen M, Ligon KL, Rowitch DH, Stiles CD: The central nervous system-restricted transcription factor Olig2 opposes p53 responses to genotoxic damage in neural progenitors and malignant glioma. *Cancer Cell* 2011, 19:359–371
75. Agarwal ML, Agarwal A, Taylor WR, Stark GR: p53 controls both the G2/M and the G1 cell cycle checkpoints and mediates reversible

- growth arrest in human fibroblasts. *Proc Natl Acad Sci U S A* 1995, 92:8493–8497
76. Fajac A, Da Silva J, Ahomadegbe JC, Rateau JG, Bernaudin JF, Riou G, Benard J: Cisplatin-induced apoptosis and p53 gene status in a cisplatin-resistant human ovarian carcinoma cell line. *Int J Cancer* 1996, 68:67–74
77. Wei Q, Dong G, Yang T, Megyesi J, Price PM, Dong Z: Activation and involvement of p53 in cisplatin-induced nephrotoxicity. *Am J Physiol Renal Physiol* 2007, 293:F1282–F1291
78. Molitoris BA, Dagher PC, Sandoval RM, Campos SB, Ashush H, Fridman E, Brafman A, Faerman A, Atkinson SJ, Thompson JD, Kalinski H, Skaliter R, Erlich S, Feinstein E: siRNA targeted to p53 attenuates ischemic and cisplatin-induced acute kidney injury. *J Am Soc Nephrol* 2009, 20:1754–1764
79. Eltabbakh GH, Belinson JL, Kennedy AW, Biscotti CV, Casey G, Tubbs RR, Blumenson LE: p53 overexpression is not an independent prognostic factor for patients with primary ovarian epithelial cancer. *Cancer* 1997, 80:892–898
80. de Graeff P, Crijns AP, de Jong S, Boezen M, Post WJ, de Vries EG, van der Zee AG, de Bock GH: Modest effect of p53, EGFR and HER-2/neu on prognosis in epithelial ovarian cancer: a meta-analysis. *Br J Cancer* 2009, 101:149–159
81. Strobel T, Swanson L, Korsmeyer S, Cannistra SA: BAX enhances paclitaxel-induced apoptosis through a p53-independent pathway. *Proc Natl Acad Sci U S A* 1996, 93:14094–14099
82. Stubbert LJ, Smith JM, McKay BC: Decreased transcription-coupled nucleotide excision repair capacity is associated with increased p53- and MLH1-independent apoptosis in response to cisplatin. *BMC Cancer* 2010, 10:207
83. Basu A, Krishnamurthy S: Cellular responses to cisplatin-induced DNA damage. *J Nucleic Acids* 2010, 2010:201367
84. Lawrenson K, Gayther SA: Ovarian cancer: a clinical challenge that needs some basic answers. *PLoS Med* 2009, 6:e25
85. Espinosa I, Catasus L, Canet B, D'Angelo E, Munoz J, Prat J: Gene expression analysis identifies two groups of ovarian high-grade serous carcinomas with different prognosis. *Mod Pathol* 2011, 2011:11
86. Taniguchi T, Tischkowitz M, Ameziane N, Hodgson SV, Mathew CG, Joenje H, Mok SC, D'Andrea AD: Disruption of the Fanconi anemia-BRCA pathway in cisplatin-sensitive ovarian tumors. *Nat Med* 2003, 9:568–574
87. Solovei I, Kreysing M, Lanctot C, Kosem S, Peichl L, Cremer T, Guck J, Joffe B: Nuclear architecture of rod photoreceptor cells adapts to vision in mammalian evolution. *Cell* 2009, 137:356–368
88. Elcock LS, Bridger JM: Exploring the relationship between interphase gene positioning, transcriptional regulation and the nuclear matrix. *Biochem Soc Trans* 2010, 38(Pt 1):263–267
89. Hawryluk-Gara LA, Shibuya EK, Wozniak RW: Vertebrate Nup53 interacts with the nuclear lamina and is required for the assembly of a Nup93-containing complex. *Mol Biol Cell* 2005, 16:2382–2394
90. Pickersgill H, Kalverda B, de Wit E, Talhout W, Fornerod M, van Steensel B: Characterization of the *Drosophila melanogaster* genome at the nuclear lamina. *Nat Genet* 2006, 38:1005–1014
91. Guelen L, Pagie L, Brasset E, Meuleman W, Faza MB, Talhout W, Eussen BH, de Klein A, Wessels L, de Laat W, van Steensel B: Domain organization of human chromosomes revealed by mapping of nuclear lamina interactions. *Nature* 2008, 453:948–951